Mohamed Tanta, J. G. Pinto, Vítor Monteiro, Antonio P. Martins, Adriano S. Carvalho and João L. Afonso

"A Comprehensive Comparison of Rail Power Conditioners Based on Two-level Converters and a V/V Power Transformer in Railway Traction Power Systems"

In the 7th Transport Research Arena (TRA 2018) Conference, 16-19 April 2018, pp.1-10, Vienna, Austria.

DOI: 10.5281/zenodo.1483284

VIENNA 2018 TRA
TRANSPORT RESEARCH ARENA
A digital era for transport
solutions for society, economy and environment

Mohamed Tanta, J. G. Pinto, Vítor Monteiro, Antonio P. Martins, Adriano S. Carvalho and João L. Afonso "A Comprehensive Comparison of Rail Power Conditioners Based on Two-level Converters and a V/V Power Transformer in Railway Traction Power Systems". In the 7th Transport Research Arena (TRA 2018), 16-19 April 2018, p.p 1-10, Vienna, Austria.

Proceedings of 7th Transport Research Arena TRA 2018, April 16-19, 2018, Vienna, Austria

A Comprehensive Comparison of Rail Power Conditioners Based on Two-level Converters and a V/V Power Transformer in Railway Traction Power Systems

Mohamed Tanta[a*], J. G. Pinto[a], Vítor Monteiro[a], Antonio. P. Martins[b], Adriano. S. Carvalho[b] and João. L. Afonso[a]

[a]*Centro ALGORITMI – University of Minho, Campus de Azurém , 4800-058, Guimarães – Portugal*
[b]*SYSTEC Research Center – University of Porto, Rua Roberto Frias, 4200-465, Porto – Portugal*

Abstract

Electric locomotives in the traction power systems represent huge nonlinear single-phase loads and they affect adversely the public electrical grid stability and the power quality. Some of such problems are related to the harmonic distortion and the Negative Sequence Components (NSCs). The Rail Power Conditioners (RPCs) are widely used to accomplish harmonics mitigation, besides NSCs compensation, then, maintaining balanced and sinusoidal public electrical grid currents. This paper presents a comprehensive comparison study between three different RPCs based on the two-level converters and a V/V power transformer. The Four-Wire Rail Power Conditioner (FW-RPC), the Three-Wire Rail Power Conditioner (TW-RPC) and the Half-Bridge Rail Power Conditioner (HB-RPC) are the main conditioners of interest. The main contribution of this paper is to perform a comprehensive comparison between the aforementioned RPCs, including the control algorithms and the compensating performance regarding the power quality problems. Simulation results with different operation scenarios are presented to establish an appropriate comparison between the aforementioned RPCs topologies.

Keywords: Four-Wire Rail Power Conditioner (FW-RPC); Harmonics; Half-Bridge Rail Power Conditioner (HB-RPC); Negative Sequence Component (NSC); Power Quality; Three-Wire Rail Power Conditioner (TW-RPC).

* Corresponding author. Tel.: +351 253 510 392; fax: +351 253 510 189.
E-mail address: mtanta@dei.uminho.pt

1. Introduction

From the beginning of railway electrification, power quality improvement was a major factor to obtain an efficient traction power system in terms of operating costs and power system stability. Therefore, many research projects have been dedicated in the last decades for power quality enhancement when using the rail electrification (Perin et al., 2015). The high-speed electric locomotives, nowadays, are using the single-phase alternating current (AC) traction power system for the long-distance electrification. Many countries in Europe, as Finland and Portugal, are using the single-phase 25 kV, 50 Hz AC power system for the high-speed trains. Other countries, like Austria and Germany, are using the single-phase 15 kV, 16.7 Hz AC power system for the high-speed traction applications (Krastev et al., 2016). However, as long as the electric locomotives are huge single-phase loads connected to the three-phase public electrical grid through several single-phase traction power transformers, this leads to power quality deterioration of the three-phase public electrical grid. Consequently, several adverse influences will affect directly the public electrical grid performance (Langerudy et al., 2017). Fig. 1 shows the single-phase traction power transformers to interface between the three-phase public electrical grid and the single-phase traction electrical grid. However, this typical connection contributes to a poor power quality on the three-phase public electrical grid side, because it does not totally solve the problem of currents imbalance (Perin et al., 2015).

Power quality term indicates a wide area of parameters, such as voltage and current imbalance, harmonics, voltage fluctuations (sags and swells), reactive power, etc. The most challenging ones, in case of electrified railways, are the harmonic currents and the Negative Sequence Components (NSCs) of currents resulting from the three-phase currents imbalance (Gazafrudi et al., 2015). Consequently, poor power quality leads to higher power losses, less power system efficiency and higher operating costs for the electric locomotives. In order to overcome the above-mentioned drawbacks and to improve the public electrical grid power quality, power electronic conditioners nowadays are a proficient solution.

The Rail Power Conditioner (RPC) is one of the power electronics systems to suppress the locomotives negative effects on the three-phase public electrical grid side, thus, maintaining balanced public grid currents without NSCs and with reduced Total Harmonic Distortion (THD) (Luo et al., 2011). Usually, The RPC system consists of a V/V power transformer (or a Scott power transformer) and power converters connected between two load sections through step-down coupling transformers. The load sections are separated by a catenary neutral section as shown in Fig. 2 (Gazafrudi et al., 2015). Considering the different possible scenarios, this paper presents a comprehensive and comparative study between three different RPC topologies based on the two-level converters and a V/V power transformer with two load sections (discontinuous catenary line with a neutral section) for 25 kV, 50 Hz traction power systems.

The first topology is the Four-Wire Rail Power Conditioner (FW-RPC), which consists of two single-phase full-bridge back-to-back converters, sharing the same DC-link with eight power switches (IGBTs) (Luo et al., 2011). The second topology is the Three-Wire Rail Power Conditioner (TW-RPC), which consists of three legs and six power switches, where one of the legs is connected directly to the grounded wire of the two single-phase load sections voltages (Wu et al., 2012). The last topology under comparison is the Half-Bridge Rail Power Conditioner (HB-RPC), which consists of two single-phase half-bridge converters connected by two capacitors in series and a grounded midpoint (Ma et al., 2013). The RPCs topologies under comparison in this study are shown in the Fig. 3.

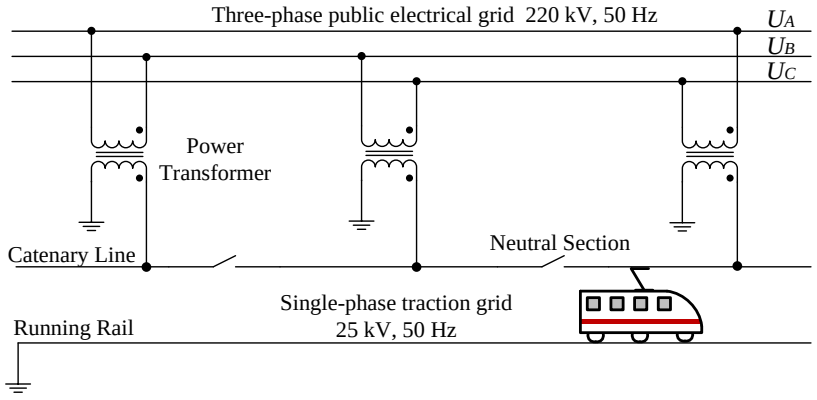

Fig. 1. Using single-phase power transformers with neutral sections to alternate between public electrical grid phases.

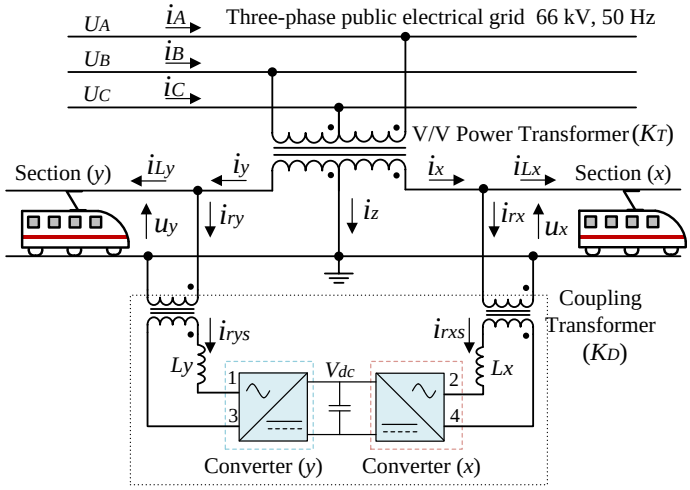

Fig. 2. RPC connection with a V/V power transformer in electrified railways systems.

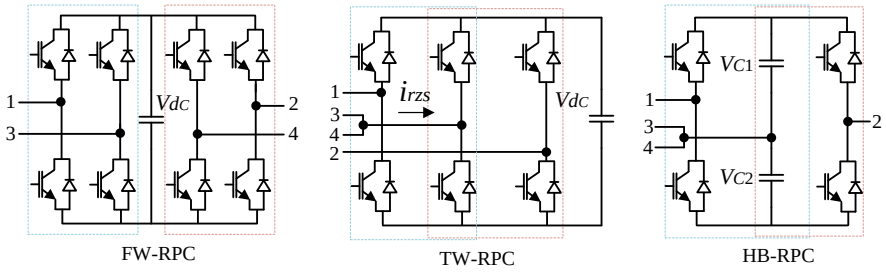

Fig. 3. RPCs topologies based on two-level converters.

Over the last few years, it has been noticed that railways substations have grown in use of RPC systems for the economic use of the public electrical grid. However, a comparative study between FW-RPC, TW-RPC, and the HB-RPC was not enough clarified in the literature. In this context, the main contributions of this paper are related with a detailed and a comprehensive comparison about the aforementioned RPCs topologies, as well as the control algorithms and the public electrical grid power quality in terms of harmonic currents and NSCs when using each topology individually. Section II and section III present in details the indicated RPCs topologies and the respective control algorithms. Section IV presents the simulation results with different operation scenarios to establish an efficient comparison between the topologies, taking into consideration the case of a load variation with time to evaluate the performance of each topology. Section V presents the main compensators characteristics and the advantages/disadvantages of using each RPC topology. Finally, section VI presents the main conclusions of this work.

2. RPC Compensation Principle

The main objective of RPC scheme is to compensate the NSCs and the harmonic currents on the three-phase public electrical grid side. However, power quality issues on the load section sides of electrified railways were not under interest by scholars because the traction load has a poor power quality by nature (Gazafrudi et al., 2015). Consequently, the majority of power quality studies in electrified railways systems are focusing on the power quality improvement of the three-phase public electrical grid side.

In this study, load sections voltages U_x and U_y have the value of 25 kV, 50 Hz and they are in phase with the corresponded line voltages U_{AC} and U_{BC}, respectively, as presented in equation (1), where K_T is the turns ratio of the V/V power transformer. Before turning on the RPC system and after assuming the power factor of the two load sections is nearly 1, the load currents for both load sections I_{Lx}, I_{Ly} are in phase with U_{AC} and U_{BC} respectively. By another meaning, I_x, I_y currents on the secondary side of the V/V power transformer and I_A, I_B currents on the primary side of the V/V power transformer are in phase with U_{AC} and U_{BC} line voltages, as shown in the phasor diagram of Fig. 4 (a).

$$U_x = U_{AC} / K_T , \quad U_y = U_{BC} / K_T \tag{1}$$

The RPC main task is to balance between the public electrical grid currents I_A, I_B, I_C, in order to eliminate the effects of NSCs of currents. This is possible by compensating both of the active and the reactive power. The RPC

shifts a quantity of half the active load power difference from the fully loaded section (in our study, section *x*) to the partially loaded section (in our study, section *y*) (Tanta et al., 2017a). In this case, the currents after shifting the active power difference are equal to I_{A1}, I_{B1} and I_{C1} as shown in the Fig. 4 (b), the equations (2) and (3). The difference between the load sections currents I_{Lx}, I_{Ly} and the phase currents I_x, I_y should be generated by the RPC, called the compensation currents I_{rx}, I_{ry}. The currents I_{rxa} and I_{rya} are the active components of the compensation currents injected by the RPC.

$$\dot{I}_{A1} = \dot{I}_A + \dot{I}_{rxa1}\ , \quad \dot{I}_{B1} = \dot{I}_B + \dot{I}_{rya1}\ , \quad \dot{I}_{C1} = -\dot{I}_{A1} - \dot{I}_{B1} \tag{2}$$

$$\dot{I}_A = \frac{\dot{I}_{Lx}}{K_T}\ , \quad \dot{I}_B = \frac{\dot{I}_{Ly}}{K_T} \tag{3}$$

$$I_{rxa1} = \frac{I_{rxa}}{K_T} = \frac{1}{2\,K_T}\,(I_{Lx} - I_{Ly}), \quad I_{rya1} = \frac{I_{rya}}{K_T} = \frac{1}{2\,K_T}\,(I_{Lx} - I_{Ly})$$

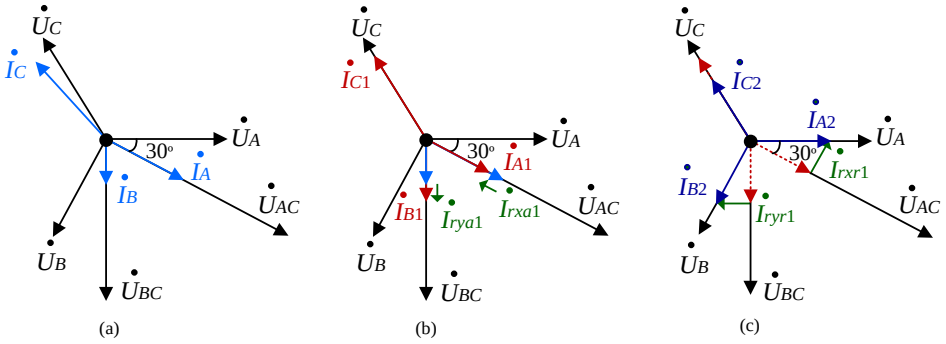

Fig. 4. RPC phasors: (a) Before compensation; (b) After active power compensation; (c) After active and reactive power compensation.

The currents after shifting the active power are still imbalanced, then, a quantity of reactive power should be compensated by the RPC (Luo et al., 2011; Wu et al., 2012). The converter (*x*) compensates a quantity of a capacitive reactive power ($\dot{I}_{rxr1}$ leads the voltage $\dot{U}_{AC}$), while the converter (*y*) compensates a quantity of an inductive reactive power ($\dot{I}_{ryr1}$ lags the voltage $\dot{U}_{BC}$) because section (*x*) has a bigger load than the one in section (*y*). The final currents after compensating both of the active and the reactive power are presented in the equation (4) and in the Fig. 4 (c).

$$\dot{I}_{A2} = \dot{I}_{A1} + \dot{I}_{rxr1}\ , \quad \dot{I}_{B2} = \dot{I}_{B1} + \dot{I}_{ryr1} \tag{4}$$

$$I_{rxr1} = \frac{I_{rxr}}{K_T} = \frac{1}{2\,K_T}\,(I_{Lx} + I_{Ly})\,\tan\frac{\pi}{6}\ , \quad I_{ryr1} = \frac{I_{ryr}}{K_T} = \frac{1}{2\,K_T}\,(I_{Lx} + I_{Ly})\,\tan\frac{\pi}{6} \tag{5}$$

3. RPC Control Algorithm

The control algorithm of the RPC should give the orders to inject the compensation currents, then acquiring sinusoidal and symmetrical currents on the public electrical grid side without NSCs. In this context, and from the equations (2) and (3), the equation (6) gives the public electrical grid currents values after only shifting the active power difference from the highly loaded section to the lightly loaded one.

$$\dot{I}_{A1} = \frac{I_{Lx} + I_{Ly}}{2\,K_T}\,e^{-j30}\ , \quad \dot{I}_{B1} = \frac{I_{Lx} + I_{Ly}}{2\,K_T}\,e^{-j90} \tag{6}$$

The previous equations (4), (5) and (6) give the final values of the public electrical grid currents after compensation. The currents, in this case, are balanced and have the same magnitude as in equation (7).

$$\dot{I}_{A2} = \frac{1}{\sqrt{3}\,K_T}\,(I_{Lx} + I_{Ly})\,e^{j0}\ , \quad \dot{I}_{B2} = \frac{1}{\sqrt{3}\,K_T}\,(I_{Lx} + I_{Ly})\,e^{-j120}\ , \quad \dot{I}_{C2} = \frac{1}{\sqrt{3}\,K_T}\,(I_{Lx} + I_{Ly})\,e^{j120} \tag{7}$$

The instantaneous values of the load sections currents can be used to obtain the peak values of the public electrical grid currents after compensation, as in the equation (8) (Luo et al., 2011).

$$i_{Lx} = I_{Lxam}\sin(\omega t - 30) + I_{Lxrm}\sin(\omega t - 120) + \sum_{h=2}^{\infty} i_{Lxh}$$
$$i_{Ly} = I_{Lyam}\sin(\omega t - 90) + I_{Lyrm}\sin(\omega t - 180) + \sum_{h=2}^{\infty} i_{Lyh} \quad (8)$$

The active and the reactive peak current components of load section (x) are respectively, I_{Lxam} and I_{Lxrm}. The h^{th} order of the instantaneous harmonic currents of load section (x) is the current i_{Lxh}. The same is applicable for the load section (y) instantaneous current equation. Multiplying the instantaneous values of i_{Lx} and i_{Ly} by $\sin(\omega t - 30)$ and $\sin(\omega t - 90)$, respectively, gives the peak values of I_{x2}, I_{y2} after filtering the signals by using a low pass filter (LPF) and multiplying the signal by $2/\sqrt{3}$, as shown in the Fig. 5. The instantaneous phase currents after compensation i_{x2}, i_{y2} are acquired after multiplying the peak values with the correspondent sine waveforms. The final reference currents i^*_{rx}, i^*_{ry} are calculated according to equation (9). The final reference currents are multiplied by K_D, the turns ratio of the coupling transformers (Joseph and Thomas, 2014; Luo et al., 2011).

$$i^*_{rx} = i_{x2} - i_{Lx}, \quad i^*_{ry} = i_{y2} - i_{Ly}$$
$$i^*_{rxs} = K_D\, i^*_{rx}, \; i^*_{rys} = K_D\, i^*_{ry} \quad (9)$$

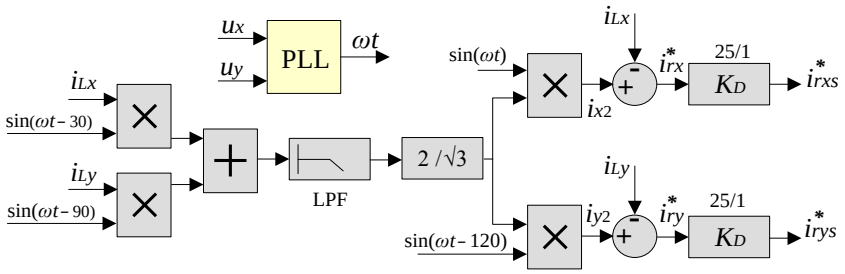

Fig. 5. Control algorithm to calculate the compensation currents references.

The RPCs topologies under interest use only high-voltage capacitors to obtain the DC-link voltage. However, a DC-link voltage control is indispensable to guarantee a good operating performance of the RPC. Fig. 6 (a) shows the DC-link voltage control for the FW-RPC topology. Only one proportional integral (PI) controller is used to correct the error between the reference value of the DC-link voltage $V_{dc,ref}$ and the instantaneous actual value v_{dc}. The output of this PI controller is multiplied by $\sin(\omega t - 30)$ and $\sin(\omega t - 90)$ to obtain two signals synchronized with i^*_{rxs}, i^*_{rys}. Two PI controllers are used to correct the error between the actual and the reference value of the compensation currents. Then, a Pulse Width Modulation (PWM) technique is used to drive the power switches (Langerudy and Mariscotti, 2016).

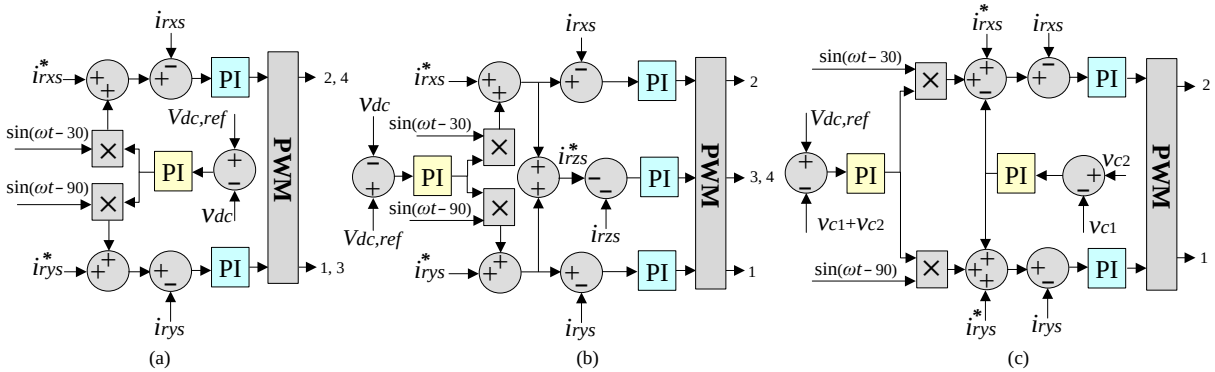

Fig. 6. DC-link voltage control and PWM modulation: (a) FW-RPC; (b) TW-RPC; (c) HB-RPC.

The TW-RPC topology has the same DC-link voltage control as shown in the Fig. 6 (b). However, three PI controllers are used to drive the power switches by using PWM technique. The DC-link voltage control of the HB-RPC topology requires a PI controller to equalize the voltage between v_{c1} and v_{c2}. Additional PI controller is used to follow the reference value of the DC-link voltage $V_{dc,ref}$. Two PI controllers are used to correct the error between the actual and the reference value of the compensation currents (Kaleybar et al., 2013).

4. Simulation Results

The simulation models for the FW-RPC, TW-RPC and HB-RPC have developed by using the *PSIM* software for power electronics simulation. In order to make a real comparative case study between the aforementioned RPCs, the simulation models will contain varied loads values to study the dynamic response of each RPC, besides some other characteristics. A common electrical traction system was selected as a case study with model parameters as shown in Table 1. The arbitrary full nominal load value for each load section is equal to 3.7 MW, where the loading summary during the simulation is presented in Table 2. The RPC is turned on after 0.2 second and when both of the load sections (*x*) and (*y*) were fully loaded. The RPCs topologies are compared by using stationary optimized PI controllers that guarantee an efficient performance between topologies. The RPCs were tuned properly at their best configuration and setting points, where the optimized PI controllers decrease the error of the DC-link voltage, besides minimizing the variations of the DC-link voltage during the transient states.

Table 1. Simulation model parameters.

Parameters	Symbol	Values FW-RPC, TW-RPC, HB-RPC	Unit
Public electrical grid voltage	U_{AC}, U_{BC}	66	kV
Traction electrical grid voltage	U_x, U_y	25	kV
DC-link capacitor initial voltage	$V_{dc,\ initial}$	2.5	kV
Turns ratio of V/V transformer	K_T	2.65	-
Turns ratio of coupling transformer	K_D	25	-
Traction electrical grid frequency	f	50	Hz
IGBTs Switching frequency	f_{sw}	10	kHz
DC-link capacitance	C_{dc}	100	mF
Converter line inductance	L_x, L_y	1	mH

Table 2. Load sections values during the simulation.

Time (second)	0.1 → 0.2	0.2 → 0.4	0.4 → 0.6	0.6 → 0.8	0.8 → 1
Section (*x*)	Full	Full	Half	Half	Half
Section (*y*)	Full	Full	Full	Half	No load
RPC	Off	On			

4.1. FW-RPC Compensator

The FW-RPC has 8 power switches and two back-to-back converters as shown in the Fig. 3. The results of the public electrical grid currents during simulation are shown in the Fig. 7 (a). The FW-RPC was turned on after 0.2 second and the currents before the indicated time (before compensation) were imbalanced. The NSCs of currents had the biggest value before compensation, which harmfully affect the power quality of the public electrical system.

The FW-RPC started to compensate the NSCs of currents after 0.2 second. Consequently, public electrical grid currents were balanced and the NSC waveform was significantly decreased as shown in Fig. 7 (b). As a result of NSC decrement, the Positive Sequence Component (PSC) will increase to reach the Root Mean Square (RMS) value of the public electrical grid currents. The PSC and NSC currents vectors of the public electrical grid at the fundamental frequency 50 Hz are calculated by using equation (10) (Ladniak, 2014). The zero sequence component of currents has no value in the electrified railways systems as long as the traction transformers do not have the fourth wire (Gazafrudi et al., 2015; Ladniak, 2014).

$$\dot{PSC} = \frac{1}{3}\left(\dot{I}_A + \alpha\,\dot{I}_B + \alpha^2\,\dot{I}_C\right), \quad \dot{NSC} = \frac{1}{3}\left(\dot{I}_A + \alpha^2\,\dot{I}_B + \alpha\,\dot{I}_C\right); \quad \alpha = e^{j120},\ \alpha^2 = e^{j240} \tag{10}$$

Fig. 7 (c) shows the compensation currents i_{rx}, i_{ry}, which are provided by the FW-RPC to compensate both of the active and the reactive power as in the phasor diagram of Fig. 4. The RPC performance is closely influenced by the DC-link voltage stability during each operation scenario. For instance, and as shown in the Fig. 7 (d), the DC-link capacitor was charged during the period between 0.2 and 0.4 second. Therefore, currents waveforms during that period had the highest NSCs ratio among the subsequent periods. After 0.4 second, the DC-link voltage

was constant during each case study and the NSCs ratio was remarkably reduced. The DC link voltage control of the FW-RPC is shown in the Fig. 6 (a).

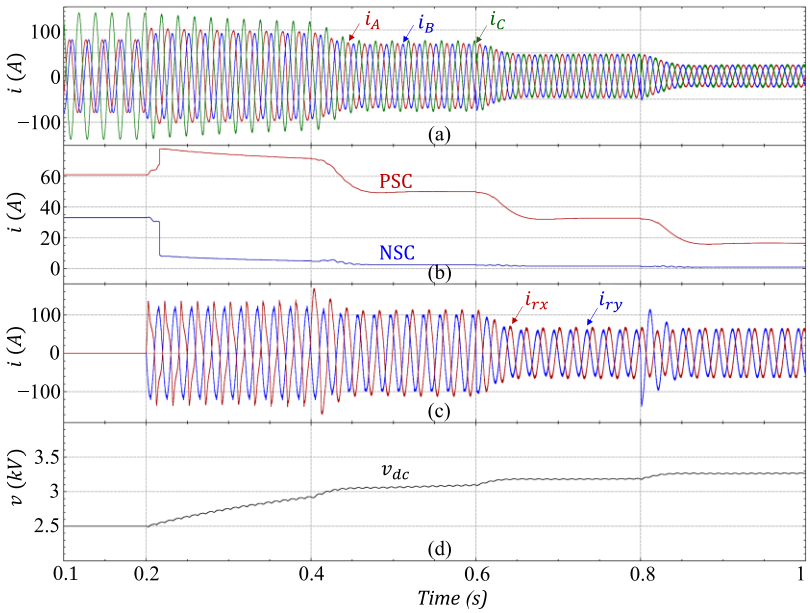

Fig. 7. FW-RPC simulation results: (a) Public electrical grid currents during the simulation; (b) PSCs and NSCs of public electrical grid currents; (c) Compensation currents provided by the FW-RPC; (d) DC-link voltage of FW-RPC.

The active power waveforms for the FW-RPC are shown in the Fig. 8. The total input active power that is consumed by the load sections and the compensator is shown in the Fig. 8 (a). The load sections power varies during the simulation, as shown in the Fig. 8 (b) and the Table 2. All the RPCs topologies have the ability to shift half of the load active power difference from the highly loaded section to the lightly loaded one. Consequently, Fig. 8 (c) demonstrates the shifted active power difference which is provided by the highly loaded section converter to the lightly loaded section converter. For instance, in the period between 0.4 and 0.6 second, the load section (*y*) was fully loaded with 3.7 MW (P_{Ly} waveform) and section (*x*) was loaded with the half of the full load (P_{Lx} waveform). As a result, the active power should be provided by section (*y*) converter (negative waveform) to be consumed by section (*x*) converter in the period between 0.4 and 0.6 second. The negative waveform of P_{cy} refers to the direction of the active power from section (*y*) converter to section (*x*) converter.

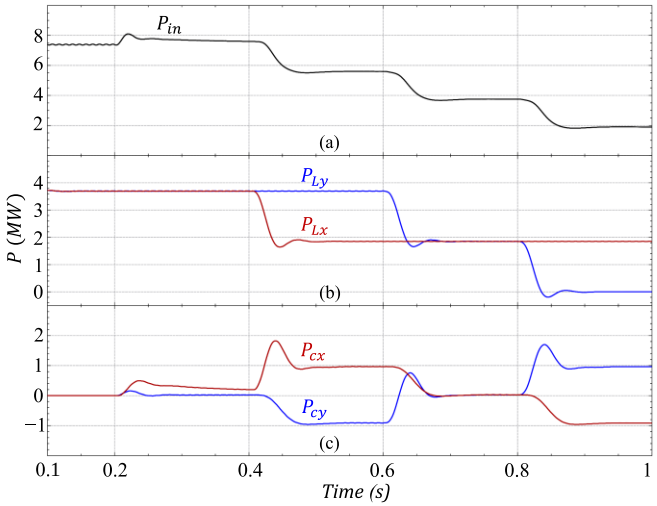

Fig. 8. Active power waveforms: (a) Total consumed power from the public electrical grid (input power); (b) Load sections active power; (c) Active power provided / consumed by the FW-RPC converters.

4.2. TW-RPC Compensator

The TW-RPC consists of 6 power switches assuming a three-phase current controlled converter with a single DC-link capacitor as shown in Fig. 3. The control algorithm and the DC-link voltage control are shown in Fig. 5 and Fig. 6 (b), respectively. The simulation model parameters of TW-RPC has exactly the values indicated in

Table 1, besides the loading conditions values for both load sections indicated in Table 2. Simulation results of the public electrical grid currents are shown in the Fig. 9 (a). The currents are balanced after 0.2 second and the compensation currents provided by the compensator i_{rx}, i_{ry}, i_{rz}, are shown in Fig. 9 (c). The DC-link voltage performance in Fig. 9 (d) is almost similar to the one of the FW-RPC. The results show a better dynamic performance of the TW-RPC than the FW-RPC topology and at the same operation conditions.

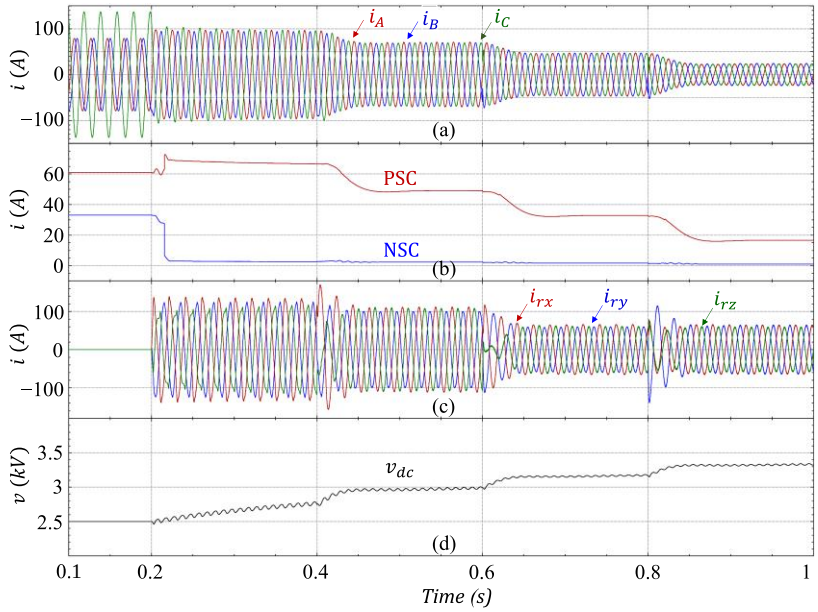

Fig. 9. TW-RPC simulation results: (a) Public electrical grid currents during the simulation; (b) PSCs and NSCs of public electrical grid currents; (c) Compensation currents provided by the TW-RPC; (d) DC-link voltage of TW-RPC.

4.3. HB-RPC Compensator

The HB-RPC contains only 4 power switches to generate the compensation currents. However, in order to feed the same traction load with a nominal power of 3.7 MW, the DC-link voltage should be 100% larger than the other types of RPC compensators as shown in the Fig. 10 (d). In addition, the DC-link of the HB-RPC is formed by two capacitors in series with a grounded center-split midpoint. The voltage stress on the HB-RPC power switches is two times the voltage stress of the FW-RPC and the TW-RPC. The high value of the stored energy in the HB-RPC DC-link capacitors ensures a good dynamic response of the compensator to match the same dynamic performance of the FW-RPC and TW-RPC compensators.

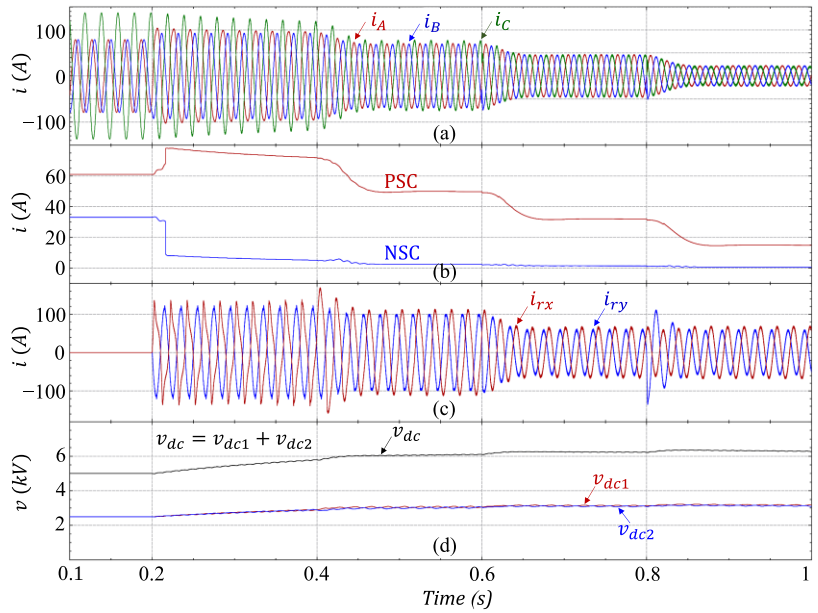

Fig. 10. HB-RPC simulation results: (a) Public electrical grid currents during the simulation; (b) PSCs and NSCs of public electrical grid currents; (c) Compensation currents provided by the HB-RPC; (d) DC-link voltages of HB-RPC.

5. RPCs Compensators Evaluation

The power quality issues (NSCs and harmonics in the case under study) are the main significant part in the selection process of the RPC topologies in the electrified railways systems. In order to evaluate the RPCs performance, Table *3* shows the NSCs ratio of the public electrical grid currents before compensation ($0.1 \rightarrow 0.2$) and after compensation ($0.2 \rightarrow 1$). The values indicated in Table 3 are presented in the steady state after the transient. The NSC ratio before compensation is almost half of the PSC of public grid side currents (51%), then the public grid power quality is highly deteriorated. After 0.2 second, the RPC compensator is turned on and the NSC ratio is significantly reduced to 7.2% or less. The FW-RPC has a more robust performance than the TW-RPC when only one load section was loaded ($0.8 \rightarrow 1$), while the NSCs ratio has increased in the same period when using the TW-RPC. In the rest of the periods, the FW-RPC and the TW-RPC have a similar performance regarding the NSCs compensation. The HB-RPC compensating performance is highly related to the DC-link voltage value, where during the period of the lowest load value ($0.8 \rightarrow 1$), it gives the best performance among the other compensators.

Table 3. NSCs ratio in the public electrical grid currents for the studied RPCs during simulation (NSC/PSC %).

Time (second)	**0.1 → 0.2**	**0.2 → 0.4**	**0.4 → 0.6**	**0.6 → 0.8**	**0.8 → 1**
FW-RPC		5.7%	3.9%	3.7%	4%
TW-RPC	51%	3.9%	3.6%	4%	4.9%
HB-RPC		7.2%	3.9%	3.4%	3.1%

Among the studied RPCs topologies, the TW-RPC is the favored in terms of performance and the total costs, since it has the same FW-RPC compensating capability with less 2 power switches. In addition, TW-RPC requires less space for installation comparing to the FW-RPC topology as shown in Table 4. The voltage stress, current stress and the equivalent switching frequency of IGBTs have the same values in both topologies of FW-RPC and TW-RPC. Consequently, similar factors and conditions are considered in the selection process of power switches.

The HB-RPC seems to be the cheapest option as it only requires four power switches. However, the tradeoff here is between the cost and the performance. Other aspects should be in consideration when choosing the HB-RPC compensator. For example, the equivalent switching frequency would decrease by 50%, which can increase the high-frequency currents harmonic contents (Ma et al., 2013). Furthermore, the voltage stress for each power switch would be double (2 p.u.; per unit), which determines to use switches with a higher voltage stress capability. Moreover, the DC-link voltage is usually selected to be 100% larger than other RPC topologies to improve the dynamic performance and to guarantee a reliable operation of the HB-RPC (Tanta et al., 2017b). The required power switches with a higher voltage stress, besides the required high voltage DC-link with two capacitors in series and the control complexity could make the total costs of the HB-RPC are similar to the ones of the TW-RPC. The DC-link capacitors are not very cheap and the required power switches with a higher voltage stress are more expensive. Also, and after a long time, the capacitors (namely electrolytic capacitors) are more subject to power failures and have an expected lifetime shorter than the power switches. Consequently, the reliability of the HB-RPC will diminish and will be adversely affected over time.

Table 4. Comparing the main characteristics between the studied RPC topologies.

RPC	**Power switches (IGBTs) characteristics**				**DC-link voltage**	**Control complexity**	**Costs**	**Space utilization**
	IGBTs number	**Equivalent switching frequency**	**Voltage stress**	**Current stress**				
FW-RPC	8	$2\ f_{sw}$	1 p.u.	1 p.u.	1 p.u.	*	***	***
TW-RPC	6	$2\ f_{sw}$	1 p.u.	1 p.u.	1 p.u.	**	**	**
HB-RPC	4	f_{sw}	2 p.u.	1 p.u.	2 p.u.	***	*/**	*

6. Conclusion

This paper reviews three different Rail Power Conditioner (RPC) topologies based on two-level power electronics converters and a V/V power transformer, in 25 kV, 50 Hz electrified railways systems. The RPC compensator is mainly used to suppress the Negative Sequence Components (NSCs) of currents on the public electrical grid side,

which are the main reason for power quality deterioration. The Four-Wire RPC (FW-RPC), the Three-Wire RPC (TW-RPC) and the Half-Bridge RPC (HB-RPC) are evaluated through the simulation models to study the general characteristics and performance of each topology. The same parameters are used during the simulation and the RPCs were adjusted properly at their best configuration and setting points to ensure an effective comparison between the indicated RPCs. The control algorithm for each RPC is also presented as a part of this comparative study. The simulation results show the compensating performance of RPCs at the same operation conditions. All the indicated RPCs have the ability to compensate the NSCs and to improve the public grid power quality. However, the TW-RPC is the recommended RPC among the other topologies in terms of costs and performance, because it requires less power switches (IGBTs) than the FW-RPC, maintaining the same performance and other aspects (e.g., voltage stress, current stress and switching frequency of IGBTs). The results show that many factors should be considered when selecting the HB-RPC for power quality improvements when using the electrified railways systems. Although the HB-RPC only needs half of the FW-RPC IGBTs, which is advantageous in terms of costs, it has some drawbacks in terms of IGBTs voltage stress, higher DC-link voltage, besides the control complexity. Moreover, the equivalent switching frequency is reduced by 50% when using the HB-RPC topology, which can increase the high-frequency currents harmonic contents, thus causing some deterioration in the power quality of the public electrical grid.

Acknowledgements

Mohamed Tanta was supported by FCT (Fundação para a Ciência e Tecnologia) PhD grant with a reference PD/BD/127815/2016. This work has been supported by COMPETE: POCI-01-0145–FEDER–007043 and FCT within the Project Scope: UID/CEC/00319/2013.

References

Gazafrudi, S.M.M., Langerudy, A.T., Fuchs, E.F., and Al-Haddad, K. (2015). Power Quality Issues in Railway Electrification: A Comprehensive Perspective. IEEE Trans. Ind. Electron. *62*, 3081–3090.

Joseph, V.P., and Thomas, J. (2014). Power quality improvement of AC railway traction using railway static power conditioner a comparative study. In 2014 International Conference on Power Signals Control and Computations (EPSCICON), pp. 1–6.

Kaleybar, H.J., Farshad, S., Asadi, M., and Jalilian, A. (2013). Multifunctional control strategy of Half-Bridge based Railway Power Quality Conditioner for Traction System. In 2013 13th International Conference on Environment and Electrical Engineering (EEEIC), pp. 207–212.

Krastev, I., Tricoli, P., Hillmansen, S., and Chen, M. (2016). Future of Electric Railways: Advanced Electrification Systems with Static Converters for ac Railways. IEEE Electrification Mag. *4*, 6–14.

Ladniak, L. (2014). Calculation of voltage unbalance factor in power system supplying traction transformers. In 2014 Power Systems Computation Conference, pp. 1–5.

Langerudy, A.T., and Mariscotti, A. (2016). Tuning of a railway power quality conditioner. In 2016 18th Mediterranean Electrotechnical Conference (MELECON), pp. 1–7.

Langerudy, A.T., Mariscotti, A., and Abolhassani, M.A. (2017). Power Quality Conditioning in Railway Electrification: A Comparative Study. IEEE Trans. Veh. Technol. *66*, 6653–6662.

Luo, A., Wu, C., Shen, J., Shuai, Z., and Ma, F. (2011). Railway Static Power Conditioners for High-speed Train Traction Power Supply Systems Using Three-phase V/V Transformers. IEEE Trans. Power Electron. *26*, 2844–2856.

Ma, F., Luo, A., Xu, X., Xiao, H., Wu, C., and Wang, W. (2013). A Simplified Power Conditioner Based on Half-Bridge Converter for High-Speed Railway System. IEEE Trans. Ind. Electron. *60*, 728–738.

Perin, I., Nussey, P.F., Cella, U.M., Tran, T.V., and Walker, G.R. (2015). Application of power electronics in improving power quality and supply efficiency of AC traction networks. In 2015 IEEE 11th International Conference on Power Electronics and Drive Systems, pp. 1086-1094.

Tanta, M., Afonso, J.A., Martins, A.P., Carvalho, A.S., and Afonso, J.L. (2017a). Rail Power Conditioner Based on Indirect AC/DC/AC Modular Multilevel Converter Using a Three-phase V/V Power Transformer. In World Congress on Engineering WCE 2017 Conference, (London, UK), pp. 289–294.

Tanta, M., Monteiro, V., Pinto, G., Exposto, B., Martins, A.P., Nogueiras Meléndez, A., Carvalho, A.S., and Afonso, J.L. (2017b). Simplified Rail Power Conditioner Based on a Half-Bridge Indirect AC/DC/AC Modular Multilevel Converter and a V/V Power Transformer. In the 43rd Annual Conference of the IEEE Industrial Electronics Society (IES) IECON 2017 (Beijing, China), (accepted for publication).

Wu, C., Luo, A., Shen, J., Ma, F.J., and Peng, S. (2012). A Negative Sequence Compensation Method Based on a Two-Phase Three-Wire Converter for a High-Speed Railway Traction Power Supply System. IEEE Trans. Power Electron. *27*, 706–717.